Localized $4f$ States and Dynamic Jahn-Teller Effect in PrO_2

A. T. Boothroyd,[1] C. H. Gardiner,[1] S. J. S. Lister,[1] P. Santini,[1] B. D. Rainford,[2] L. D. Noailles,[3] D. B. Currie,[4] R. S. Eccleston,[5] and R. I. Bewley[5]

[1]*Department of Physics, University of Oxford, Oxford, OX1 3PU, United Kingdom*
[2]*Department of Physics, University of Southampton, Southampton, SO17 1BJ, United Kingdom*
[3]*Inorganic Chemistry Laboratory, University of Oxford, Oxford, OX1 3QR, United Kingdom*
[4]*Department of Chemistry, University of Southampton, Southampton, SO17 1BJ, United Kingdom*
[5]*ISIS Facility, Rutherford Appleton Laboratory, Chilton, Didcot, OX11 0QX, United Kingdom*

(Received 1 September 2000)

Neutron spectroscopic measurements of the magnetic excitations in PrO_2 reveal (1) sharp peaks characteristic of transitions between levels of the $4f^1$ configuration of Pr^{4+} split by the cubic crystal field, and (2) broad bands of scattering centered near 30 and 160 meV. We present a simple model based on a vibronic Hamiltonian that accounts for these contrasting features of the data. The analysis shows that 90% $\pm$ 10% of the Pr ions have a localized $4f^1$ configuration and provides strong evidence for a dynamic Jahn-Teller effect in the Γ_8 electronic ground state.

DOI: 10.1103/PhysRevLett.86.2082 PACS numbers: 71.28.+d, 71.70.Ch, 71.70.Ej, 78.70.Nx

Anomalous static and dynamic magnetic properties of rare earth and actinide compounds containing strongly correlated electrons are usually attributed to Kondo or valence fluctuations, or to the formation of heavy fermion states. If, however, there are unquenched orbital degrees of freedom, then other mechanisms for anomalous behavior are possible. One such mechanism is the coupling of electronic charge fluctuations to phonons, and leads to magnetoelastic and Jahn-Teller phenomena. In the case of localized electrons the dynamic Jahn-Teller effect (DJTE) may quench electronic degrees of freedom, causing a reduction in the magnetic moment and forming states of mixed magnetic and phonon character [1].

Electron-lattice effects of this kind are, of course, well known, but the absence of a clean DJTE system has undoubtedly hindered their identification among other anomalous properties, especially in Ce and U compounds. In this Letter we show that PrO_2 represents such a model DJTE system. We find that magnetoelastic coupling has a dramatic influence on the static and dynamic properties of PrO_2, and we provide the first direct measurements of the magnetovibrational spectrum in a rare earth DJTE compound. We also show that the Pr ions exist almost entirely in a localized $4f^1$ configuration, in disagreement with an intermediate valence model for PrO_2.

PrO_2 is an insulator with the fluorite structure type. It exhibits type-I antiferromagnetic ordering below $T_N = 14$ K with an anomalously low ordered moment of $\sim 0.6\mu_B$ [2]. The electronic ground state of PrO_2 has, together with the other fluorite-structure lanthanide dioxides CeO_2 and TbO_2, been controversial for many years [3–6]. Core-level photoabsorption and photoemission spectra have been interpreted by some authors [3,4] in terms of an intermediate valence ground state composed of a roughly 50:50 admixture of localized (i.e., atomiclike) $4f^1$ and $4f^2$ states. Others [5,6], however, believe in a localized $4f^1$ configuration with a degree of covalent mixing such that the oxygen $2p$ valence band contains some extended states of f symmetry. Publication of an influential model [7] describing an intermediate valence state in the anomalous cuprate $PrBa_2Cu_3O_{6+x}$ (PrBCO) similar to that proposed for the lanthanide dioxides has increased interest in PrO_2, making it a key reference compound in high energy spectroscopic studies of PrBCO [8] and related materials.

The aim of the present work was to clarify the electronic ground state of PrO_2. Neutron spectroscopy is a powerful tool for studying the electronic structure of rare earths because it probes electronic transitions within the ground state configuration both within and between the $^{2S+1}L_J$ terms, including splittings due to the crystalline electric field (CEF) or exchange fields. The low neutron energies ($\lesssim 1$ eV) and weak coupling to the electronic angular momentum ensure that final state effects are insignificant. The experiments were performed on the high energy transfer (HET) chopper spectrometer at the ISIS Facility. On HET neutrons of well-defined incident energy E_i are delivered to the sample in short pulses. Spectra are recorded as a function of flight time in banks of detectors surrounding the incident beam direction. Because the spectra are recorded at constant scattering angle ϕ, the scattering vector Q varies with energy E; thus $\hbar^2 Q^2/2m = 2E_i - E - 2\cos\phi\sqrt{E_i(E_i - E)}$.

Polycrystalline samples of PrO_2 were prepared by oxidation of commercially obtained Pr_6O_{11}. The starting material was baked in air at 1000 °C for several hours and then annealed either in flowing O_2 at 280 °C for approximately 20 days or under 300–500 atm pressure of O_2 at 350 °C for 3–5 days. The products were checked by x-ray diffraction and no trace of residual Pr_6O_{11} could be detected. From this, and a comparison of our neutron data with that of Pr_6O_{11} [9], we estimate an upper limit of 1% on the amount of Pr_6O_{11} impurity in our samples.

 0031-9007/01/86(10)/2082(4)$15.00

For the neutron measurements approximately 10 g of PrO_2 was wrapped in aluminum foil and mounted in contact with the cold head of a closed-cyle refrigerator. Data were collected with $E_i = 30$, 180, 450, 750, and 1200 meV, and the scattering from vanadium was used to normalize the spectra and to convert them into units of absolute scattering cross section. The presented spectra correspond to the partial differential cross section $d^2\sigma/d\Omega\, dE_f$ multiplied by the factor k_i/k_f [10], where k_i and k_f are the initial and final neutron wave vectors and E_f is the final energy. Measurements were made under identical conditions on a 10 g sample of polycrystalline CeO_2 in order to estimate the nonmagnetic (phonon + multiple scattering) background in the PrO_2 data. CeO_2 is an almost ideal material for this purpose as it has the same structure as PrO_2 and the scattering cross sections of Pr and Ce differ by only 10%. The estimated transmission of the PrO_2 and CeO_2 samples was 93%–97% (depending on E and E_i), and the spectra were corrected accordingly.

Figure 1(a) shows spectra of PrO_2 and CeO_2 with $E_i = 180$ meV averaged over the angular ranges 9°–19° ($\langle\phi\rangle = 14°$) and 125°–139° ($\langle\phi\rangle = 133°$). At high angles the scattering is dominated by one-phonon processes, and so the 133° data measures the phonon density of states weighted by the neutron cross section of the atoms. The 133° data for the two compounds are similar except that some PrO_2 peaks are shifted to lower energies relative to CeO_2, most noticeably below 30 meV. At low angles more marked differences are observed. The PrO_2 data contains a sharp peak at 131 meV and a broad peak centered on ~30 meV extending from 10 to 80 meV, whereas the CeO_2 spectrum shows little structure and lies below the PrO_2 spectrum at all energies. The 131 meV peak has been observed previously [2]. Both the broad and sharp peaks in the PrO_2 data decrease in intensity with increasing Q consistent with a typical $4f$ magnetic form factor, and so we identify these features as magnetic in origin. Conversely, the CeO_2 signal systematically increases in intensity with Q, and this implies that the CeO_2 scattering is nonmagnetic as expected for a $4f^0$ configuration with no admixture of localized $4f^1$ states.

Several other magnetic features were observed in the PrO_2 data in addition to those already described. The runs with $E_i = 750$ and 1200 meV detected two more peaks. These are shown in Figs. 1(b) and 1(c). The peak centered near 350 meV in the 750 meV run is significantly broader than the resolution, whereas the peak centered at 730 meV in the 1200 meV run is resolution limited. The 450 meV run revealed a shoulder of scattering above the 131 meV peak, centered at ~160 meV. This feature is displayed in the inset of Fig. 1(d). Finally, the $E_i = 30$ meV run revealed a peak centered at 3 meV shown in Fig. 1(d). This peak shifted to lower energies as the temperature was raised, becoming quasielastic above ~15 K. Given that $T_N = 14$ K we can confidently attribute this 3 meV peak to spin wave excitations of the antiferromagnetically ordered ground state. We found no evidence in our data for an excitation at 5.4 meV reported in a previous work [11], and so we conclude that this feature is not intrinsic to PrO_2.

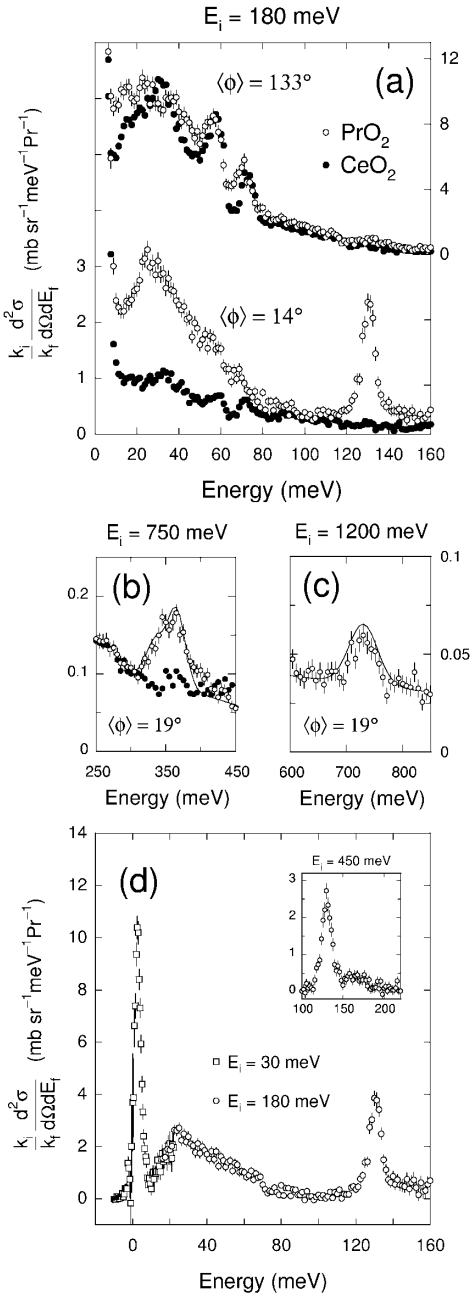

FIG. 1. Neutron inelastic scattering from PrO_2 and CeO_2 measured at a temperature of 10 K. In (a) the incident neutron energy E_i was 180 meV, and spectra recorded at low and high scattering angles are shown. (b),(c) show $^2F_{5/2} \rightarrow {}^2F_{7/2}$ intermultiplet transitions PrO_2 measured with $E_i = 750$ and 1200 meV, respectively. The solid lines are cross sections calculated from the CEF model described in the text with widths corresponding to the instrumental resolution. (d) Data corrected for the nonmagnetic background and the Q dependence of the magnetic cross section as described in the text. Main frame: $E_i = 30$ and 180 meV. Inset: $E_i = 450$ meV showing the shoulder to the 131 meV peak.

Figure 1(d) shows data from several runs after correction for the nonmagnetic scattering and for the calculated (see below) magnetic form factor. The form factor correction extrapolates the data to zero Q and hence allows comparison of runs with different incident energies.

We begin our interpretation of the results by considering the effect of the CEF. The splitting of a localized $4f^1$ configuration in a cubic CEF is described by the spin-orbit coupling constant ζ, which sets the $^2F_{5/2} \rightarrow {}^2F_{7/2}$ separation, and the fourth and sixth order CEF parameters B_0^4 and B_0^6. Using the free ion value of ζ for Pr^{4+} [12] Kern *et al.* [13] have calculated the energy levels as a function of the ratio B_0^6/B_0^4. They assigned the 131 meV peak to the $\Gamma_8 \rightarrow \Gamma_7$ transition of $^2F_{5/2}$, and by estimating the ratio B_0^6/B_0^4 from a point charge model they arrived at a parametrization of the CEF. The model of Kern *et al.* predicts the levels in the CEF-split $^2F_{7/2}$ term to be $\sim$320 meV (Γ_6'), $\sim$390 meV (Γ_8'), and $\sim$580 meV (Γ_7') above the ground state in rough accord with the peaks in Figs. 1(b) and 1(c). We conclude, therefore, that these high energy peaks arise from the $^2F_{5/2} \rightarrow {}^2F_{7/2}$ intermultiplet transitions, the only proviso being that the signal in Fig. 1(b) must encompass both the Γ_6' and Γ_8' levels. Assuming this to be the case, we refined the CEF model with the 14 states $|J; m_J\rangle$ of $^2F_{5/2}$ and $^2F_{7/2}$ as a basis. With all three parameters allowed to vary independently, the fitting procedure converged yielding $B_0^4 = (-776 \pm 8)$ meV, $B_0^6 = (207 \pm 5)$ meV, and $\zeta = (100.5 \pm 1)$ meV [14] and gave excellent agreement with the observed energies.

With the eigenfunctions from the CEF refinement we can now evaluate the cross sections for the observed transitions as a function of Q. The formulas [10] contain radial moments of the $4f$ wave function, and values of these for Pr^{4+} were taken from Ref. [15]. The curve in Fig. 1(b) represents the calculated cross sections for the $\Gamma_8 \rightarrow \Gamma_6'$ and $\Gamma_8 \rightarrow \Gamma_8'$ transitions, and the curve on Fig. 1(c) is likewise for the $\Gamma_8 \rightarrow \Gamma_7'$ transition. Considering that no additional parameters are needed to obtain the calculated cross sections the level of agreement with the data is very good. The same cannot be said, however, when the cross sections for the $\Gamma_8 \rightarrow \Gamma_8$ and $\Gamma_8 \rightarrow \Gamma_7$ transitions are calculated. At zero Q these are 182 and 99 mb sr^{-1} Pr^{-1}, respectively [16], considerably greater than the integrated spectral weights 47 and 48 mb sr^{-1} Pr^{-1} in the 3 and 131 meV peaks shown in Fig. 1(d) [17].

We will now describe a model that both accounts for the puzzling intensities just mentioned and explains the origin of the 10–80 meV broad peak and the 160 meV shoulder. Our hypothesis is that these effects derive from a strong coupling between $4f^1$ electronic states and local dynamic lattice distortions. This coupling mixes electronic and phonon degrees of freedom and causes a dynamic Jahn-Teller effect in the Γ_8 ground state.

The existence of a DJTE in PrO_2 was, in fact, suggested some time ago to explain the factor $\sim$2 reduction in ordered moment relative to a pure Γ_8 ground state [2]. An analogous moment reduction in UO_2 had already been attributed to a DJTE [18], and so its occurrence in PrO_2 would not be a surprise. Moreover, the neutron data in Fig. 1(a) showing substantial phonon shifts in PrO_2 relative to CeO_2 provide direct evidence for a significant magnetoelastic interaction. To find out how this interaction influences the magnetic excitation spectrum we describe a simple model for the coupling of a set of CEF levels with phonons. Group theory shows that the Γ_8 CEF ground state couples in first order to local distortions of either Γ_3 or Γ_5 symmetry, and point charge calculations indicate that the coupling strengths are comparable [18]. For the sake of simplicity, however, we will restrict our model to three degenerate local distortions of Γ_5 symmetry with vibrational frequency $\omega_{\rm ph}$. We describe the magnetoelastic coupling with the Hamiltonian

$$H_{\rm ME} = g \sum_i (a_i + a_i^\dagger) O_i \,, \tag{1}$$

where g is the coupling constant, a_i and $a_i^\dagger$ are phonon annihilation and creation operators, and O_i are the Γ_5 symmetry quadrupolar operators: $O_1 = (J_y J_z + J_z J_y)/2$, $O_2 = (J_z J_x + J_x J_z)/2$, and $O_3 = (J_x J_y + J_y J_x)/2$. To investigate the ordered magnetic moment we also included a molecular exchange field interaction $H_{\rm Ex} = \mathbf{H} \cdot \mathbf{J}$. The magnitude of $\mathbf{H}$ was chosen so as to reproduce the observed 3 meV splitting of the ground state.

We take as a basis the 24 states $|\phi_n\rangle$, $n = 1, \ldots, 24$, represented by $|\Gamma_8; 0\rangle$, $|\Gamma_7; 0\rangle$, $|\Gamma_8; 1^{(i)}\rangle$, and $|\Gamma_7; 1^{(i)}\rangle$. These are products of the CEF eigenstates and the three Γ_5 phonon modes ($i = 1, 2, 3$) containing either 0 or 1 quanta $\hbar\omega_{\rm ph}$. The energy separation Δ of $|\Gamma_8; 0\rangle$ and $|\Gamma_7; 0\rangle$ is chosen so as to reproduce the observed peak at 131 meV. The vibronic states are obtained by diagonalization of the matrix $\langle\phi_{n'}|H_{\rm ME} + H_{\rm Ex}|\phi_n\rangle$, and the magnetic part of the neutron cross section is calculated from the matrix elements of $\mathbf{J}$.

We evaluated the model for a range of parameters. Small values of $\hbar\omega_{\rm ph}$ are effective at mixing $|\Gamma_8; 0\rangle$ and $|\Gamma_8; 1^{(i)}\rangle$ states creating a DJTE. The consequences are a transfer of intensity from the ground state into the phononlike states and a reduction in the ordered moment. A large $\hbar\omega_{\rm ph}$ tends to create vibronic states involving the Γ_7 CEF excitation. To illustrate these effects we plot on Fig. 2 the zero-Q energy spectrum for two parameter sets, one (I) with small and the other (II) large $\hbar\omega_{\rm ph}$. In both cases new peaks appear between the 3 and 131 meV levels. With set I there is a factor of 0.86 reduction in the ordered moment (independent of the direction of $\mathbf{H}$) and a similar decrease in the intensity of the 3 meV peak. Set II produces a smaller effect on the ordered moment and 3 meV peak, but a new feature is the signal above the 131 meV peak.

These results give us confidence that magnetoelastic coupling is responsible for the unusual energy spectrum and reduced moment of PrO_2. Because of its simplicity we cannot expect a single-frequency model to match the data perfectly. In reality there will be coupling to local

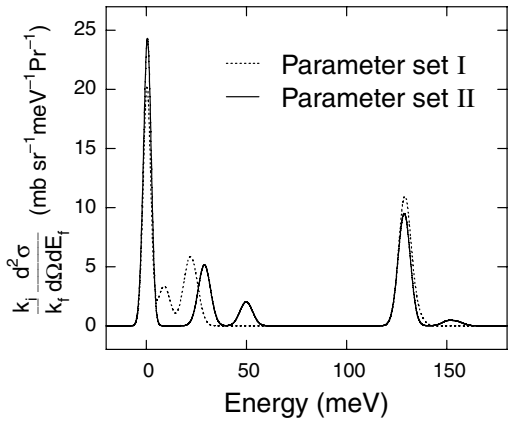

FIG. 2. Zero-Q cross section of PrO_2 calculated from the magnetoelastic model described in the text with parameter sets I ($\hbar\omega_{\rm ph} = 12.5$ meV, $g = 8$ meV, and $\Delta = 109$ meV) and II ($\hbar\omega_{\rm ph} = 42$ meV, $g = 9$ meV, and $\Delta = 101$ meV). In both cases **H** was 0.5 meV $\parallel (1,1,1)$. The peak widths correspond roughly with the experimental resolution in Fig. 1(d).

dynamic distortions with Γ_3 as well as Γ_5 symmetry, and these distortions will exist over a range of frequencies due to dispersion. The extent of the observed broad scattering is indicative that many frequencies are actually involved. A realistic model would also need to include states with >1 phonons. Nevertheless, the qualitative agreement achieved with the present model is satisfying.

Before concluding we will address the nature of the f states. Our analysis has assumed a localized $4f^1$ configuration. We can check this assumption two ways. First, we can look for the signature of localized $4f^2$ states in the range 200–300 meV where the $^3H_4 \rightarrow {}^3H_5$ transition occurs [19]. No peaks are observed. Second, we can directly determine the number of $4f^1$ states per Pr from the neutron cross section via the sum rule for transitions within a J multiplet [10]. The measured zero-Q cross section integrated up to 220 meV, including the elastic scattering [17], is 240 mb sr^{-1} Pr^{-1}. This compares with the calculated value of $182 + 99 = 281$ mb sr^{-1} Pr^{-1} for the $J = \frac{5}{2}$ multiplet [16]. Thus, by including the broad scattering in the integral we recover almost all the missing intensity. Allowing a 10% uncertainty in the absolute calibration we conclude that 90% $\pm$ 10% of the Pr ions have a localized $4f^1$ configuration. The intermultiplet transitions shown in Figs. 1(b) and 1(c) provide further support for this conclusion since the calculated cross sections based on the assumption of 100% $4f^1$ are in good agreement with the measured intensities.

In summary, our findings support a tetravalent model for PrO_2 with an almost fully occupied atomic $4f$ orbital. The neutron data allow the possibility of $\sim$10% underoccupancy relative to a pure $4f^1$ configuration, and this may indicate a degree of covalency. Any other occupied states of f symmetry must then be extended states in the O $2p$ valence band. These results rule out the strongly intermediate valence model for PrO_2, and we anticipate that a similar picture will apply to CeO_2 and TbO_2. We find compelling evidence that magnetoelastic coupling in PrO_2 creates a ground state with mixed electronic and vibrational degrees of freedom by the action of a DJTE. Being an insulator with a simple structure, localized f electrons, and a large CEF splitting, PrO_2 would seem an ideal model system for further studies of the DJTE.

We thank Mike Hayward for help with sample preparation, and the Engineering and Physical Sciences Research Council of Great Britain for financial support. P. S. thanks the Swiss NSF for financial support.

[1] I. B. Bersuker and V. Z. Polinger, *Vibronic Interactions in Molecules and Crystals* (Springer-Verlag, Berlin, 1989).
[2] S. Kern *et al.,* Solid State Commun. **49**, 295 (1984). The direction of the ordered moment is still not known.
[3] A. Kotani *et al.,* Adv. Phys. **37**, 37 (1988).
[4] A. Bianconi *et al.,* Phys. Rev. B **38**, 3433 (1988); H. Ogasawara *et al.,* Phys. Rev. B **43**, 854 (1991); S. Kimura *et al.,* J. Electron Spectrosc. Relat. Phenom. **78**, 135 (1996); S. M. Butorin *et al.,* J. Phys. Condens. Matter **9**, 8155 (1997).
[5] E. Wuilloud *et al.,* Phys. Rev. Lett. **53**, 202 (1984); F. Marabelli and P. Wachter, Phys. Rev. B **36**, 1238 (1987).
[6] R. C. Karnatak *et al.,* Phys. Rev. B **36**, 1745 (1987); H. Dexpert *et al.,* Phys. Rev. B **36**, 1750 (1987).
[7] R. Fehrenbacher and T. M. Rice, Phys. Rev. Lett. **70**, 3471 (1993).
[8] U. Neukirch *et al.,* Europhys. Lett. **5**, 567 (1988); F. W. Lytle *et al.,* Phys. Rev. B **41**, 8955 (1990); Z. Hu *et al.,* Phys. Rev. B **60**, 1460 (1999); U. Staub *et al.,* Phys. Rev. B **61**, 1548 (2000).
[9] E. Holland-Moritz, Z. Phys. B **89**, 285 (1992).
[10] S. W. Lovesey, *Theory of Neutron Scattering from Condensed Matter* (Oxford University Press, Oxford, U.K., 1984).
[11] S. Kern *et al.,* J. Appl. Phys. **67**, 4830 (1990).
[12] V. Kaufman and J. Sugar, J. Res. Natl. Bur. Stand. **71A**, 583 (1967).
[13] S.Kern *et al.,* Phys. Rev. B **32**, 3051 (1985).
[14] The B_q^k and ζ coefficients used here are defined in W. T. Carnall *et al.,* J. Chem. Phys. **90**, 3443 (1989).
[15] P. J. Brown, in *International Tables for X-ray Crystallography,* edited by A. J. C. Wilson (Kluwer Academic, Dordrecht, 1992), Vol. C; W. B. Lewis, in *Magnetic Resonance and Related Phenomena,* Proceedings of the XVIth Congress AMPERE, Bucharest, 1970, edited by I. Ursu (Publishing House of the Academy of the Socialist Republic of Romania, Bucharest, 1971), p. 717.
[16] These are somewhat smaller than the corresponding values 192 and 118 mb sr^{-1} Pr^{-1} obtained when J mixing with the $J = \frac{7}{2}$ multiplet is neglected.
[17] A further $\sim$16 mb sr^{-1} Pr^{-1} associated with elastic (Bragg) scattering from the ordered moment of $\sim 0.50\mu_B$ at 10 K is not contained in the data in Fig. 1(d).
[18] K. Sasaki and Y. Obata, J. Phys. Soc. Jpn. **28**, 1157 (1970).
[19] J. Sugar, Phys. Rev. Lett. **14**, 731 (1965).